Effect of Multiple Grooves on Aerodynamic Performance of a Low Reynolds Number UAV Propeller (Part II)

Aravind SEENI*

*Corresponding author
*Department of Aeronautical Engineering, Rajalakshmi Engineering College, Thandalam, Chennai 602 105, India,
aravindseeni.s@rajalakshmi.edu.in

DOI: 10.13111/2066-8201.2023.15.2.10

Received: 07 July 2022/ Accepted: 21 March 2023/ Published: June 2023

Abstract: *In an continuation of work previously performed by the author on grooved propellers, numerical investigations are performed on Applied Precision Composites 10×7 Slow Flyer propeller. Computational Fluid Dynamics is used to analyze the novel design. The grooved sections considered have a rectangular geometry measuring 0.1×0.1mm are placed interchangeably at 0.09c, 0.17c, 0.32c and 0.42c from the leading edge in a multi-grooved configuration i.e. more than 2 grooves. The results of the study showed that the presence of grooves had modified the flow characteristics only to detrimentally impact the thrust performance. However, the grooves improved power performance due to torque reduction. The analysis of the results showed that, in most models, low torque relative to the baseline in the operational range of the low to medium advance ratio range exists. The improvement in torque, however, did not improve efficiency in all models.*

Key Words: *passive flow control, grooved propeller, aerodynamic performance, UAV range, UAV endurance*

1. INTRODUCTION

The research described in this paper is an extension of the earlier work by the same author reported in [1], [2]. In previous published research, 17 models namely, Model−1 to Model−17 are analysed in a single grooved configuration and the performance and efficiency results reported. In this paper, the focus is to report on the results obtained for 5 additional models.

Research on improving the efficiency of UAV propellers helps to increase and add value to future applications of drones. The desired design requirement is a propelling device capable of producing improved thrust and reduced torque at a low Re. Modern research is concerned with improving the thrust through flow modifiers or flow control technique. These flow modifiers alter the fluid flow such that the flow trajectory is optimized around the aerodynamic body to attain the desired performance.

The current research is concerned with studying the flow control technique called grooved design. In the present work, a comprehensive study on grooved propeller design has been performed with the aim to study its significance for the aeronautical application. The unique features of an aeronautical propeller are low torque, high thrust and high efficiency during operation. The effect of the positioning of grooves in multiple locations on the performance characteristics of the propeller will be investigated. The positioning of multiple grooves could

have either favorable or detrimental impact on the aerodynamic performance. These have not been investigated so far and will be investigated in the current work.

2. METHODOLOGY

As in the case of earlier papers, Computational Fluid Dynamics is used to solve the governing equations of fluid flow. RANS simulations are performed with different propeller models as a first step of initiating the research on fluid dynamic analysis of grooved propeller.

2.1 Baseline propeller

Applied Precision Composites (APC) 10×7 *Slow Flyer (SF)* is considered as the baseline propeller in this study. APC10x7SF is widely used in low *Re* applications such as small-scale UAVs. This propeller is chosen based on the availability of data from the experiments of Brandt *et al.* [3].

The propeller has a diameter (*D*) of 0.254 m and pitch of 0.1778 m. Low *Re* Eppler E63 airfoil sections near the hub and thin Clark-Y air foil sections near the tip are used to design the propeller.

For the simulation, the propeller is assumed to be rotating at a constant rotational speed of 3008 rpm.

2.2 Grooved propellers

The design of propellers is performed using CAD software Catia v5. For the design of grooved propeller, baseline propeller model is modified with grooves of varying dimensions. In order to study the effect of multiple grooves, grooves of dimensions 0.1mm × 0.1mm, are placed interchangeably at different positions namely 0.09*c*, 0.17*c*, 0.32*c* and 0.42*c*. The dimensions of the grooves are varied for different positions, as listed in Table 1.

Table 1– Propeller configurations to study the effect of multiple grooves

Name	Groove size, mm	Groove position, x_{LE}
Model−24	0.1mm × 0.1mm	0.09*c*, 0.17*c*, 0.32*c*
Model−25	0.1mm × 0.1mm	0.09*c*, 0.17*c*, 0.42*c*
Model−26	0.1mm × 0.1mm	0.09*c*, 0.32*c*, 0.42*c*
Model−27	0.1mm × 0.1mm	0.17*c*, 0.32*c*, 0.42*c*
Model−28	0.1mm × 0.1mm	0.09*c*, 0.17*c*, 0.32*c*, 0.42*c*

3. RESULTS AND DISCUSSIONS

3.1 Verification and validation

The verification and validation of the model for the baseline propeller is provided in Seeni [1].

3.2 Effect of multiple grooves on propeller performance

3.2.1 Model − 24

The performance and efficiency results of Model − 24 grooved design are provided in Table 2. The relative difference between the results with baseline propeller is also listed in the table.

Table 2 – Performance and efficiency results of Model − 24

Case	Condition J	K_T	ΔK_T [%]	$10K_P$	ΔK_P [%]	η [%]	$\Delta\eta$ [%]
1	0.192	0.1068	−15.07	0.6427	−5.63	31.89	−10.16
2	0.236	0.1022	−13.43	0.6394	−3.42	37.74	−10.37
3	0.282	0.0982	−11.47	0.6234	−3.50	44.42	−8.23
4	0.334	0.0928	−9.63	0.6135	−2.47	50.53	−7.45
5	0.383	0.0856	−9.94	0.5961	−2.27	54.96	−7.78
6	0.432	0.0789	−8.77	0.5767	−1.59	59.12	−7.48
7	0.486	0.07	−6.81	0.5515	−0.28	62.91	−6.67
8	0.527	0.0636	−8.13	0.5237	−0.43	63.97	−7.82
9	0.573	0.0561	−7.59	0.4956	0.72	64.86	−8.39
10	0.628	–	–	–	–	–	–
11	0.659	0.0392	−7.91	0.4284	2.72	60.35	−10.46
12	0.717	–	–	–	–	–	–
13	0.773	–	–	–	–	–	–
14	0.799	0.0107	37.35	0.3042	20.73	28.14	13.91

Model − 24 multi-grooved design exhibited reduced K_T relative to baseline for most J analysed. For J 0.628, 0.717 and 0.773, convergence was not obtained. Therefore, the discussion will be limited to conditions where convergence was obtained. The design underperformed in terms of K_T for J 0.192 to 0.573 and 0.659. At J of 0.799, K_T improved. K_P showed decrement for J 0.192 to 0.527. For J 0.573, 0.659 and 0.799, the K_P increased relative to baseline. For J 0.192 to 0.573 and 0.659, the η was found to be reduced, ranging between −6.67% and −10.46%. Only for the high J of 0.799, the η was found to be increased at 13.91%.

The three-dimensional velocity distribution of the fluid surrounding the Model − 24 grooved propeller is modified or reduced to detrimentally affect thrust. The velocity distribution along a plane bisecting the flow field along y-z for two J case samples, 0.334 and 0.573 is shown in Fig. 1.

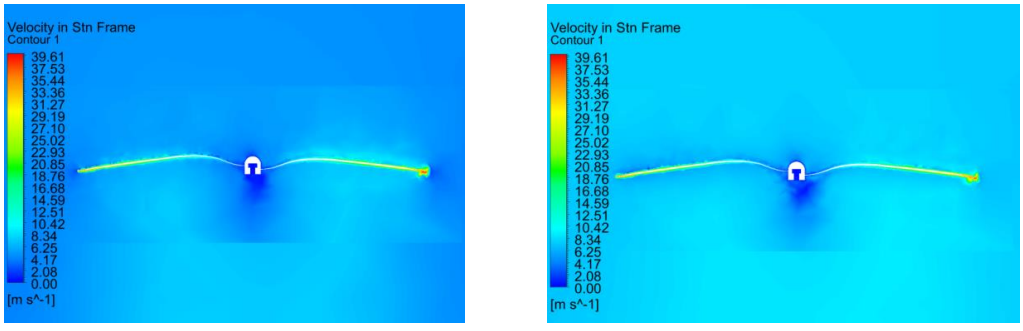

(a) (b)

Fig. 1 – Velocity flow-field around Model − 24 propeller for (a) J=0.334 and (b) J=0.573

The velocity modifications in the presence of the groove modifies the pressure distribution to affect the thrust. Lower peak pressures are maintained at the pressure side (aft) as compared to baseline whereas higher low pressures are maintained at the suction side (fore) as compared to baseline for both J=0.334 and J=0.573 cases. Fig. 2 shows the modified pressure levels on the pressure side and on the suction side in the presence of groove for two J cases, 0.334 and 0.573 when viewed along the y-z plane bisecting the flow field.

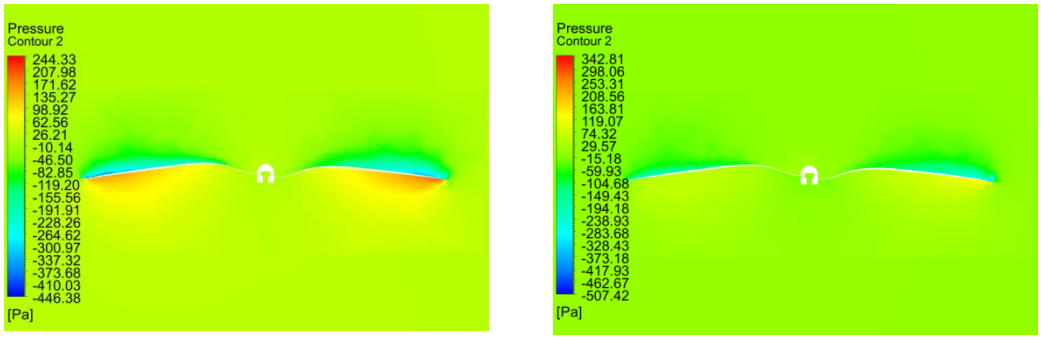

(a) (b)

Fig. 2 – Pressure contour of flow around Model−24 propeller for (a) *J*=0.334 and (b) *J*=0.573

Vector plots of fluid flow at 0.75R radial distance and velocity distribution for three-dimensional Model − 24 propeller is provided in Fig. 3 for single *J* condition *J*=0.334 to illustrate that the velocity very near to the blade surface is modified in the presence of groove.

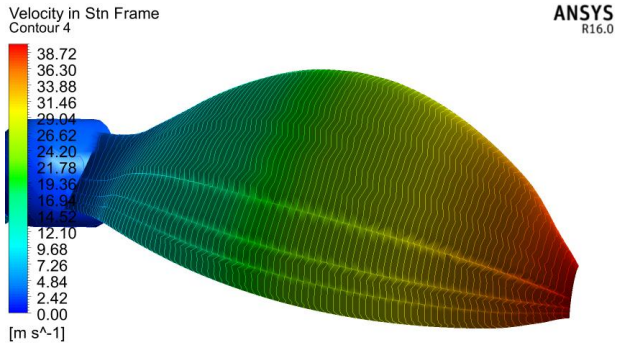

Fig. 3 – Velocity distribution on Model − 24 propeller blade for J=0.334

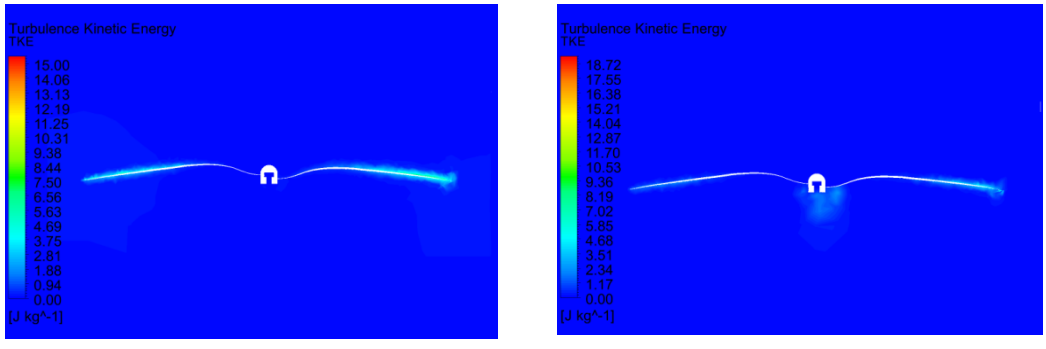

(a) (b)

Fig. 4 – Turbulence Kinetic Energy of Model − 24 propeller for (a) *J*=0.334 and (b) *J*=0.573

A measure of turbulence can be provided through Turbulence Kinetic Energy (TKE) which is a turbulence quantity.

Model − 24 grooved design has increased TKE along the blade radii compared to baseline for *J*=0.334 (Fig. 4(a)). For *J*=0.573, the TKE is increased (Fig. 4(b)).

3.2.2 Model − 25

The performance and efficiency results of Model - 25 grooved design are provided in Table 3.

Table 3 – Performance and efficiency results of Model − 25

Case	Condition J	K_T	ΔK_T [%]	$10K_P$	ΔK_P [%]	η [%]	$\Delta\eta$ [%]
1	0.192	0.1068	−15.07	0.6444	−5.38	31.81	−10.40
2	0.236	0.1027	−13.05	0.6375	−3.70	38.02	−9.70
3	0.282	0.0976	−11.96	0.6260	−3.09	43.98	−9.13
4	0.334	0.0917	−10.71	0.6115	−2.78	50.08	−8.27
5	0.383	0.0847	−10.85	0.5887	−3.50	55.10	−7.54
6	0.432	0.0782	−9.54	0.5723	−2.34	59.07	−7.56
7	0.486	0.0710	−7.36	0.5626	1.73	61.30	−9.05
8	0.527	0.0631	−8.78	0.5230	−0.58	63.61	−8.34
9	0.573	0.0546	−10.04	0.4903	−0.35	63.82	−9.85
10	0.628	–	–	–	–	–	–
11	0.659	0.0405	−4.83	0.4447	6.64	60.08	−10.86
12	0.717	0.0269	−7.32	0.3776	6.38	51.03	−12.92
13	0.773	–	–	–	–	–	–
14	0.799	0.0093	18.62	0.2950	17.08	25.06	1.44

In the case of Model − 25 multi-grooved design, numerical convergence was attained for 12 cases of J only. For J 0.628 and 0.773, the solution was not obtained. The discussion on the performance of this design henceforth will be limited to 12 cases of J. K_T for this design decreased relative to baseline for J ranging from 0.192 to 0.573, 0.659 and 0.717. For the case of J of 0.799, K_T showed a relative increase. K_P was found to be improving for the selected case of J. For J, 0.192 to 0.432, 0.572 and 0.573 the K_P decreased. For other J cases, the K_P increased relative to baseline.

The η for this multi-grooved design was observed to be decreasing for J, 0.192 to 0.573, 0.659 and 0.717. Only for the single case of 0.799 J, the design showed a marginal increase of 1.44%. The three-dimensional velocity distribution of the fluid surrounding the Model−25 grooved propeller is modified or reduced to detrimentally affect thrust. The velocity distribution along a plane bisecting the flow field along y-z for two J case samples, 0.334 and 0.573 is shown in Fig. 5.

The result shows that for J=0.334, the peak velocity is decreased compared to baseline. For J=0.573, the peak velocity remains close to baseline.

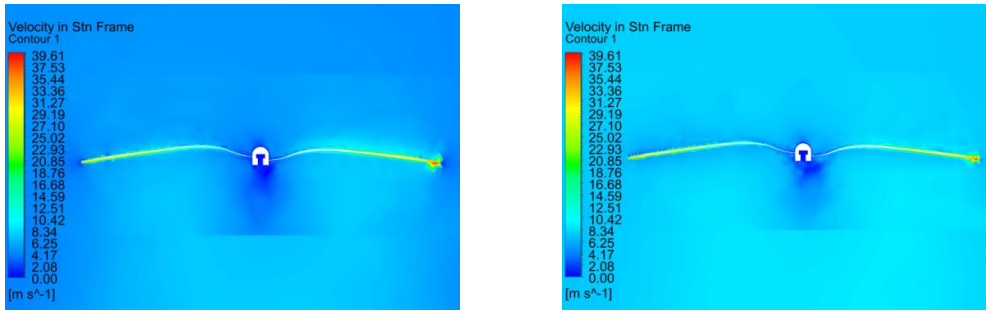

(a) (b)

Fig. 5 – Velocity flow-field around Model − 25 propeller for (a) J=0.334 and (b) J=0.573

The velocity modifications in the presence of the groove modifies the pressure distribution to affect the thrust. Lower peak pressures are maintained at the pressure side (aft) as compared to baseline whereas higher low pressures are maintained at the suction side (fore) as compared to baseline for both J=0.334 and J=0.573 cases. Fig. 6 shows the modified pressure levels on the pressure side and on the suction side in the presence of groove for two J cases, 0.334 and 0.573 when viewed along the y-z plane bisecting the flow field.

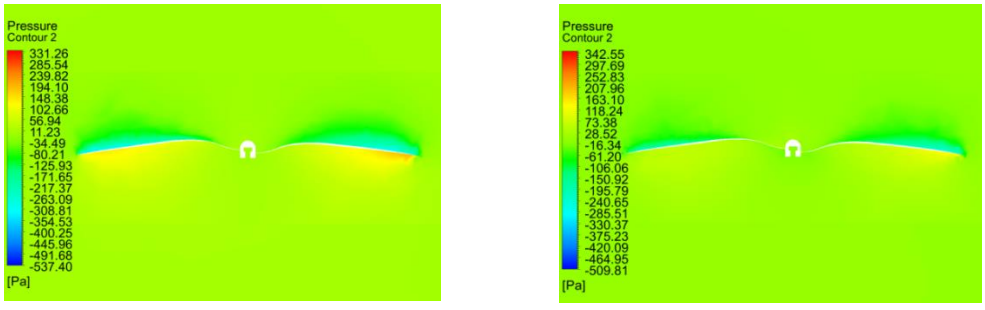

(a) (b)

Fig. 6 – Pressure contour of flow around Model−25 propeller for (a) J=0.334 and (b) J=0.573

Vector plots of fluid flow at 0.75R radial distance and velocity distribution for three-dimensional Model − 25 propeller is provided in Fig. 7 for single J condition J=0.334 to illustrate that the velocity very near to the blade surface is modified in the presence of groove.

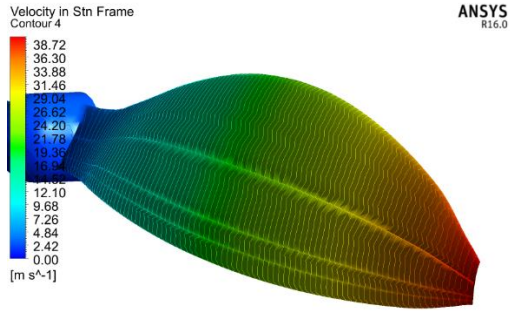

Fig. 7 – Velocity distribution on Model−25 propeller blade for J=0.334

A measure of turbulence can be provided through TKE which is a turbulence quantity. Model − 25 grooved design has increased TKE along the blade radii compared to baseline for J=0.334 and J=0.573 (Fig. 8).

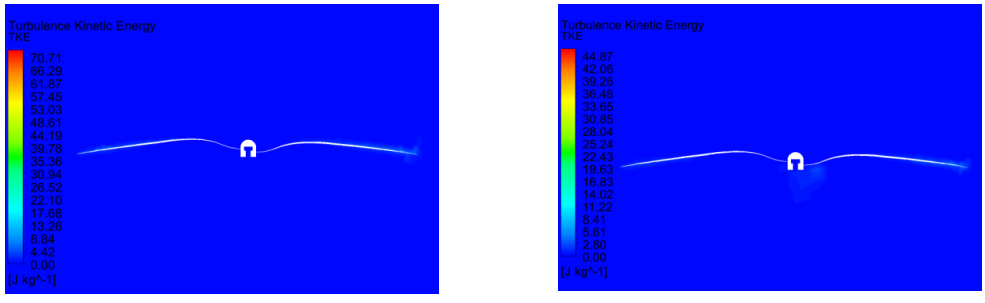

(a) (b)

Fig. 8 – Turbulence Kinetic Energy of Model − 25 propeller for (a) J=0.334 and (b) J=0.573

3.2.3 Model − 26

The performance and efficiency results of Model − 26 grooved design are provided in Table 4. The relative difference between the results with baseline propeller is also listed in the table.

For Model − 26 multi-grooved propeller design, K_T was found to be reduced for J 0.192 to 0.717. The decrement ranged between −4.70% and −14.33% for those cases of J. Only for J 0.773 and 0.799, and K_T was found to be improved. K_P was found to be decreased for J cases ranging from 0.192 to 0.486.

The decrement ranged between −1.19% and −5.52% respectively. For other J cases, 0.527 to 0.799, the K_P increased. The η was found to be decreased for all J analysed in this study. The decrement ranged between −7.5% and −15.72% for the 14 cases of J.

The three-dimensional velocity distribution of the fluid surrounding the Model−26 grooved propeller is modified or reduced to detrimentally affect thrust. The velocity distribution along a plane bisecting the flow field along y-z for two J case samples, 0.334 and 0.573 is shown in Fig. 9. The peak velocity for J=0.334 case is reduced compared to baseline. For J=0.573, the peak velocity remains closely similar to baseline.

Table 4 – Performance and efficiency results of Model−26

Case	Condition J	K_T	ΔK_T [%]	$10K_P$	ΔK_P [%]	η [%]	$\Delta\eta$ [%]
1	0.192	0.1077	−14.33	0.6434	−5.52	32.14	−9.48
2	0.236	0.1036	−12.31	0.6362	−3.89	38.42	−8.75
3	0.282	0.0966	−12.87	0.6189	−4.19	44.03	−9.03
4	0.334	0.0924	−10.08	0.6114	−2.80	50.45	−7.60
5	0.383	0.0851	−10.44	0.5925	−2.87	55.00	−7.71
6	0.432	0.0778	−10.07	0.5709	−2.57	58.86	−7.89
7	0.486	0.0700	−8.60	0.5464	−1.19	62.27	−7.62
8	0.527	0.0659	−4.70	0.5414	2.92	64.20	−7.50
9	0.573	0.0548	−9.69	0.4972	1.05	63.18	−10.77
10	0.628	0.0438	−11.22	0.4538	2.20	60.57	−13.10
11	0.659	0.0376	−11.73	0.4289	2.85	57.78	−14.27
12	0.717	0.0260	−10.25	0.3778	6.43	49.39	−15.72
13	0.773	0.0144	0.75	0.3291	16.30	33.84	−13.46
14	0.799	0.0082	5.36	0.2974	18.02	22.08	−10.62

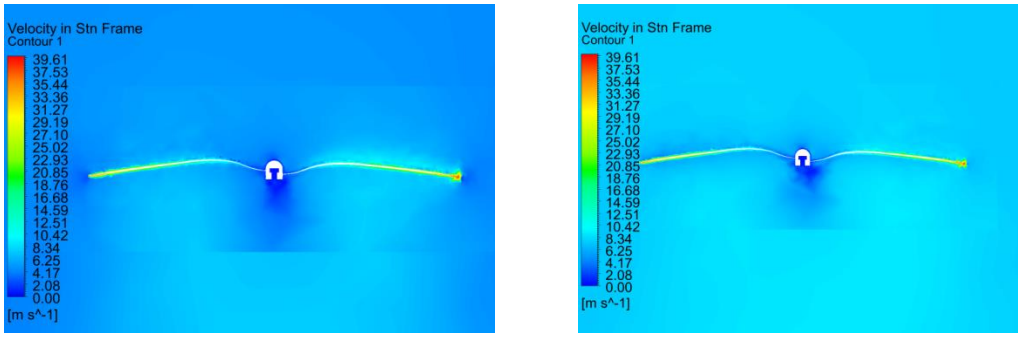

(a) (b)

Fig. 9 – Velocity flow-field around Model − 26 propeller for (a) J=0.334 and (b) J=0.573

The velocity modifications in the presence of the groove modifies the pressure distribution to affect the thrust. Lower peak pressures are maintained at the pressure side (aft) as compared to baseline whereas higher low pressures are maintained at the suction side (fore) as compared to baseline for both *J*=0.334 and *J*=0.573 cases. Fig. 10 shows the modified pressure levels on the pressure side and on the suction side in the presence of groove for two *J* cases, 0.334 and 0.573 when viewed along the y-z plane bisecting the flow field.

Vector plots of fluid flow at 0.75R radial distance and velocity distribution for three-dimensional Model − 26 propeller is provided in Fig. 11 for single *J* condition *J*=0.334 to illustrate that the velocity very near to the blade surface is modified in the presence of groove.

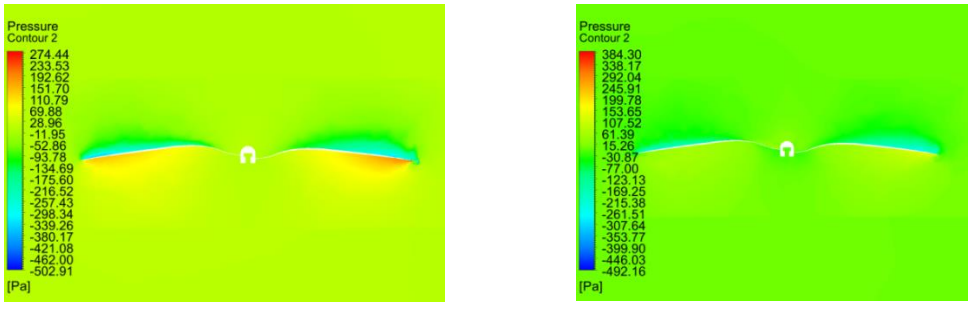

(a) (b)

Fig. 10 – Pressure contour of flow around Model − 26 propeller for (a) *J*=0.334 and (b) *J*=0.573

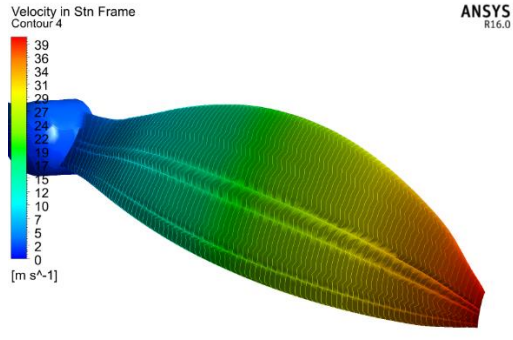

Fig. 11 – Velocity distribution on Model − 26 propeller blade for *J*=0.334

A measure of turbulence can be provided through TKE which is a turbulence quantity. Model − 26 grooved design has increased TKE along the blade radii compared to baseline for *J*=0.334 and *J*=0.573 (Fig. 12).

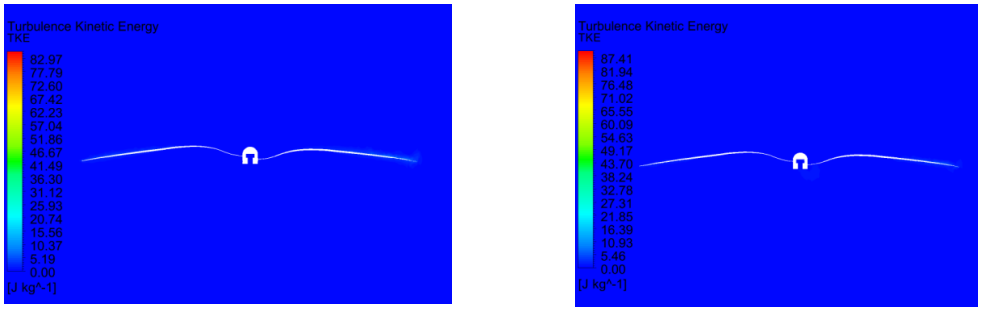

(a) (b)

Fig. 12 – Turbulence Kinetic Energy of Model − 26 propeller for (a) *J*=0.334 and (b) *J*=0.573

3.2.4 Model − 27

The performance and efficiency results of Model − 27 grooved design are provided in Table 5. The relative difference between the results with baseline propeller is also listed in the table.

Table 5 – Performance and efficiency results of Model − 27

Case	Condition J	K_T	ΔK_T [%]	$10K_P$	ΔK_P [%]	η [%]	$\Delta\eta$ [%]
1	0.192	0.1166	−7.24	0.6832	0.32	32.77	−7.70
2	0.236	0.1128	−4.48	0.6818	2.98	39.05	−7.25
3	0.282	0.1079	−2.67	0.6756	4.58	45.05	−6.92
4	0.334	0.1020	−0.67	0.6679	6.19	51.01	−6.57
5	0.383	0.0956	0.63	0.6556	7.47	55.85	−6.29
6	0.432	0.0883	2.08	0.6372	8.74	59.86	−6.32
7	0.486	0.0795	3.82	0.6122	10.71	63.13	−6.33
8	0.527	0.0725	4.75	0.5893	12.04	64.82	−6.60
9	0.573	0.0640	5.42	0.5597	13.75	65.51	−7.47
10	0.628	0.0530	7.58	0.5164	16.30	64.50	−7.46
11	0.659	0.0463	8.73	0.4897	17.42	62.34	−7.51
12	0.717	0.0336	15.69	0.4334	22.10	55.50	−5.29
13	0.773	0.0192	34.60	0.3753	32.60	39.65	1.40
14	0.799	0.0130	66.63	0.3462	37.38	30.00	21.44

Model − 27 multi-grooved design produced reduced K_T for J 0.192 to 0.334. From J of 0.383, K_T increased relative to baseline. K_P was found to be increased for all J. The increment ranged between 0.32% and 37.38%. The η was found to be reduced for all J except for 0.773 and 0.799. The three-dimensional velocity distribution of the fluid surrounding the Model−27 grooved propeller is modified or reduced to detrimentally affect thrust. The velocity distribution along a plane bisecting the flow field along y-z for two J case samples, 0.334 and 0.573 is shown in Fig. 13. For J=0.334, the peak velocity is reduced compared to baseline. For J=0.573, the peak velocity is increased.

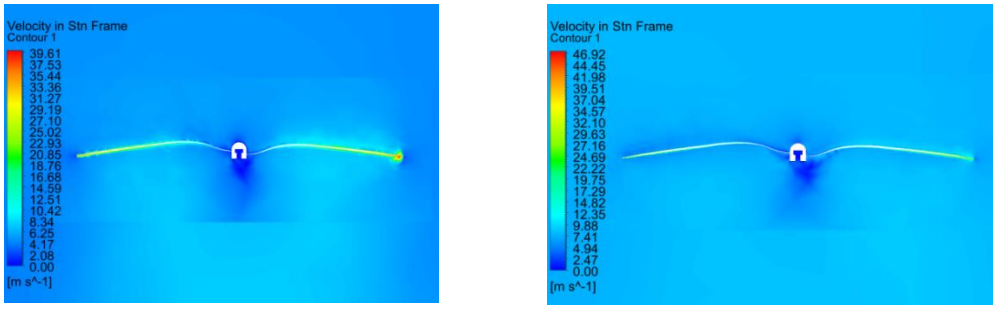

(a) (b)

Fig. 13 – Velocity flow-field around Model−27 propeller for (a) J=0.334 and (b) J=0.573

The velocity modifications in the presence of the groove modifies the pressure distribution to affect the thrust. Lower peak pressures are maintained at the pressure side (aft) as compared to baseline whereas higher low pressures are maintained at the suction side (fore) as compared to baseline for both J=0.334 and J=0.573 cases. Fig. 14 shows the modified pressure levels on the pressure side and on the suction side in the presence of groove for two J cases, 0.334 and 0.573 when viewed along the y-z plane bisecting the flow field.

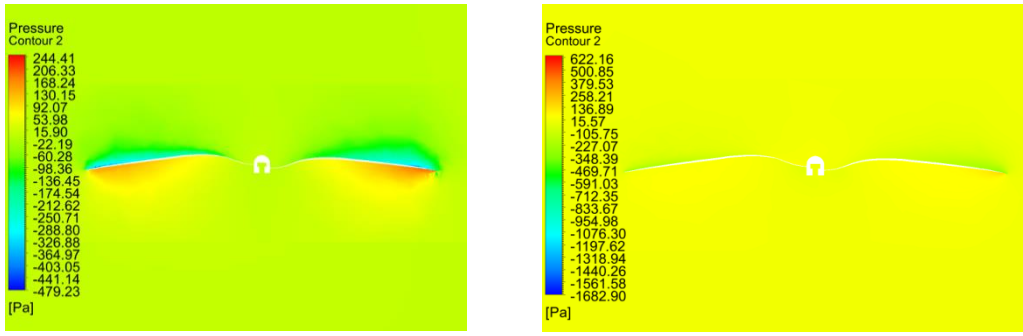

(a) (b)

Fig. 14 – Pressure contour of flow around Model − 27 propeller for (a) *J*=0.334 and (b) *J*=0.573

Vector plots of fluid flow at 0.75R radial distance and velocity distribution for three-dimensional Model − 27 propeller is provided in Fig. 15 for single *J* condition *J*=0.334 to illustrate that the velocity very near to the blade surface is modified in the presence of groove.

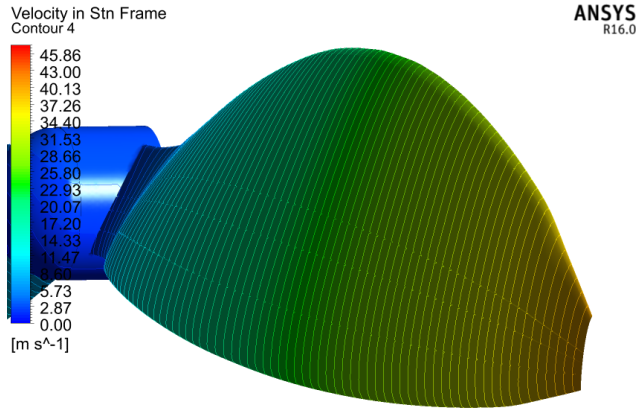

Fig. 15 – Velocity distribution on Model − 27 propeller blade for *J*=0.334

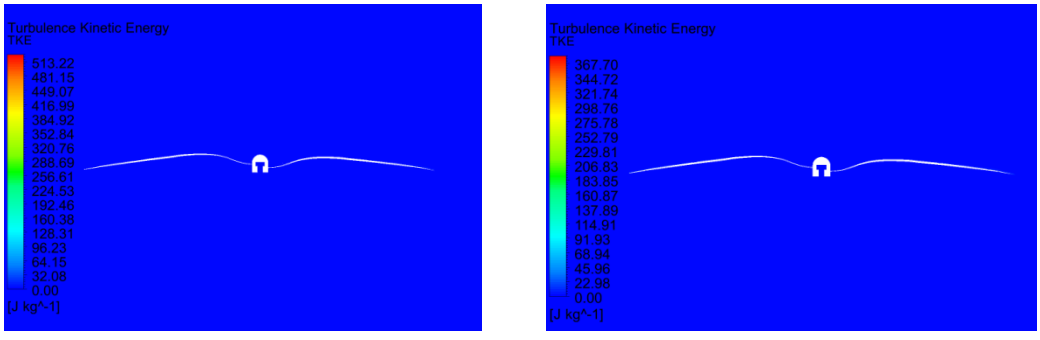

(a) (b)

Fig. 16 – Turbulence Kinetic Energy of Model − 27 propeller for (a) *J*=0.334 and (b) *J*=0.573

A measure of turbulence can be provided through TKE which is a turbulence quantity. Model − 27 grooved design has increased TKE along the blade radii compared to baseline for *J*=0.334 and *J*=0.573 (Fig. 16).

3.2.5 Model − 28

The performance and efficiency results of Model − 28 grooved design are provided in Table 6. The relative difference between the results with baseline propeller is also listed in the table.

Table 6 – Performance and efficiency results of Model − 28

Case	Condition J	K_T	ΔK_T [%]	$10K_P$	ΔK_P [%]	η [%]	$\Delta\eta$ [%]
1	0.192	0.1159	−7.76	0.6868	0.85	32.41	−8.70
2	0.236	0.1121	−5.04	0.6840	3.33	38.69	−8.10
3	0.282	0.1076	−2.96	0.6793	5.15	44.68	−7.69
4	0.334	0.1015	−1.16	0.6696	6.46	50.63	−7.27
5	0.383	0.0951	0.14	0.6563	7.60	55.51	−6.85
6	0.432	0.0880	1.68	0.6390	9.05	59.46	−6.95
7	0.486	0.0793	3.54	0.6145	11.12	62.73	−6.93
8	0.527	0.0722	4.40	0.5924	12.61	64.27	−7.39
9	0.573	0.0637	4.94	0.5618	14.19	64.96	−8.24
10	0.628	0.0527	6.91	0.5179	16.64	63.91	−8.30
11	0.659	0.0461	8.11	0.4901	17.53	61.93	−8.12
12	0.717	0.0322	11.04	0.4372	23.15	52.81	−9.87
13	0.773	0.0187	30.60	0.3751	32.54	38.49	−1.56
14	0.799	0.0127	62.48	0.3429	36.05	29.54	19.58

Model − 28 multi-grooved design was found to have reduced K_T for J 0.192 to 0.334. From J of 0.383, K_T was found to be increased. K_P was found to be increased for all J considered in the study. The η was found to be decreased for J from 0.192 to 0.773. For J of 0.799, the η was found to be increased by 19.58%.

The three-dimensional velocity distribution of the fluid surrounding the Model − 28 grooved propeller is modified or reduced to detrimentally affect thrust. The velocity distribution along a plane bisecting the flow field along y-z for two J case samples, 0.334 and 0.573 is shown in Fig. 17. For J=0.334, the peak velocity is reduced compared to baseline. For J=0.573, the peak velocity is maintained closely similar to baseline.

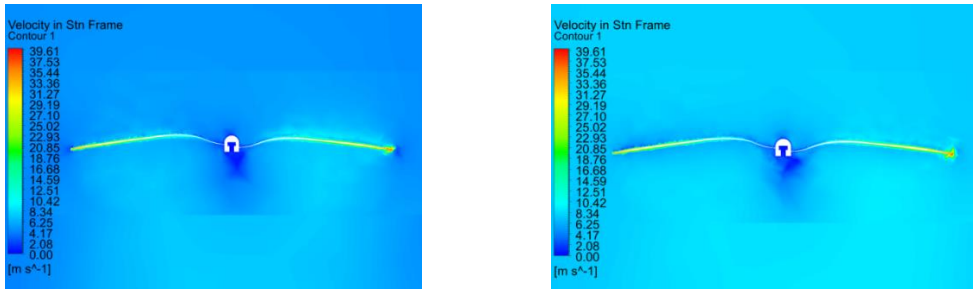

(a) (b)

Fig. 17 – Velocity flow-field around Model−28 propeller for (a) J=0.334 and (b) J=0.573

The velocity modifications in the presence of the groove modifies the pressure distribution to affect the thrust. Lower peak pressures are maintained at the pressure side (aft) as compared to baseline whereas higher low pressures are maintained at the suction side (fore) as compared to baseline for both J=0.334 and J=0.573 cases. Fig. 18 shows the modified pressure levels on the pressure side and on the suction side in the presence of groove for two J cases, 0.334 and 0.573 when viewed along the y-z plane bisecting the flow field.

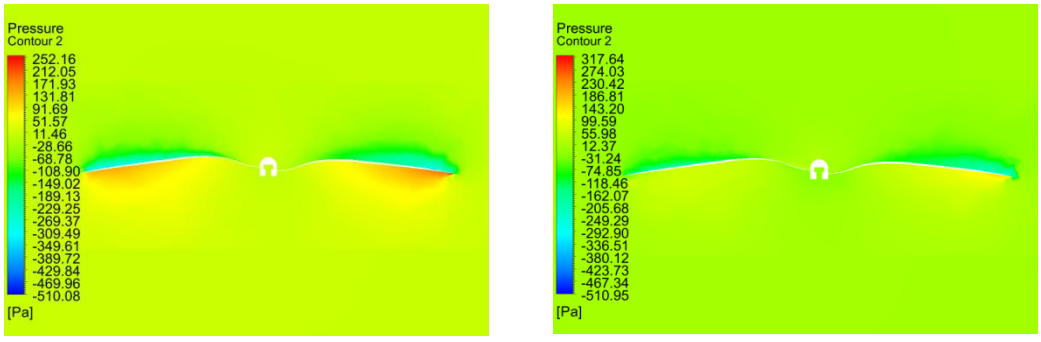

(a) (b)

Fig. 18 – Pressure contour of flow around Model − 28 propeller for (a) J=0.334 and (b) J=0.573

Vector plots of fluid flow at 0.75R radial distance and velocity distribution for three-dimensional Model − 28 propeller is provided in Fig. 19 for single J condition J=0.334 to illustrate that the velocity very near to the blade surface is modified in the presence of groove.

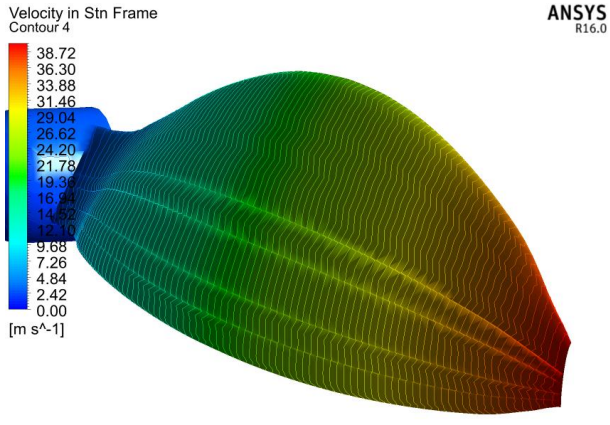

Fig. 19 – Velocity distribution on Model − 28 propeller blade for J=0.334

A measure of turbulence can be provided through TKE which is a turbulence quantity. Model − 28 grooved design has increased TKE along the blade radii compared to baseline for J=0.334 and J=0.573 (Fig. 20).

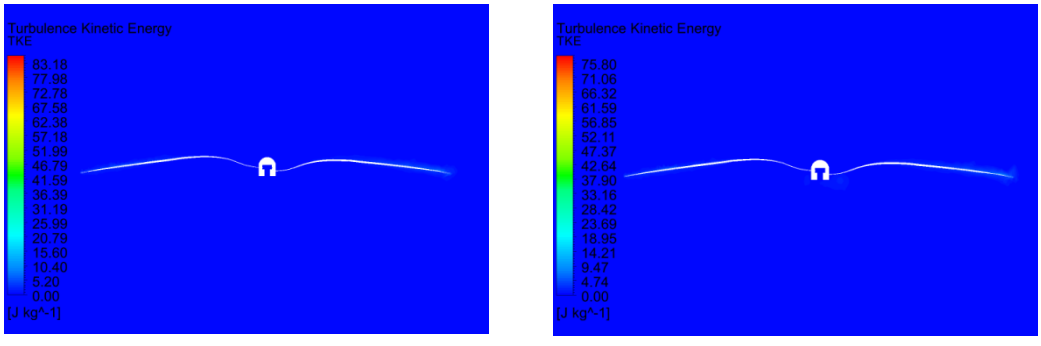

(a) (b)

Fig. 20 – Turbulence Kinetic Energy of Model − 28 propeller for (a) J=0.334 and (b) J=0.573

3.3 Implication of results for UAV flight operations

Model − 24, Model − 25 and Model − 28 grooved designs had improved η over baseline only for one J of 0.799. Model − 27 grooved design had improved η over baseline only J 0.773 and 0.799. The range of J that provides η improvement is limited. Model − 26 had no η improvement over baseline for all J. Hence these models cannot be preferred over baseline design for flight operations.

4. CONCLUSIONS

Research on grooved design implemented on a UAV propeller has been completed. A CFD investigation is conducted on propellers with different groove sizes. 5 grooved designs with cross-sections 0.1 × 0.1 mm, were studied. The performance results revealed that for 3 models, the thrust was reduced for most J between 0.192 and 0.717. For 2 models, the thrust performance was increased in the medium to higher J range, while for lower J thrust was still reduced. This implied that the presence of grooves modified the flow characteristics only to detrimentally impact the thrust performance. However, the grooves improved power performance due to torque reduction. Analysis of the K_P results showed in most of the 5 models the torque reduced compared to the baseline in the low to medium J operational range. The improvement in thrust and/or torque, however, did not contribute to improvement in η in all models. The η is the critical parameter for operation of propellers in a UAV's real-flight.

REFERENCES

[1] A. Seeni, Effect of Groove Size on Aerodynamic Performance of a Low Reynolds Number UAV Propeller, *INCAS Bulletin*, vol. **14**, no. 1, pp. 171–186, https://doi.org/10.13111/2066-8201.2022.14.1.14, 2022.
[2] A. Seeni, Effect of Groove Size on Aerodynamic Performance of a Low Reynolds Number UAV Propeller (Part II), *INCAS Bulletin*, vol. **14**, no. 4, pp. 131-144, https://doi.org/10.13111/2066-8201.2022.14.4.11, 2022.
[3] J. Brandt, R. Deters, G. Ananda, and M. Selig, Small-Scale Propeller Performance at Low Speeds – Online Database, 2010, http://www.ae.illinois.edu/m-selig/props/propDB.html (accessed May 01, 2018).